Supplemental information for:

Imaging the transition from internal to external zones of the Variscan Orogen (NW Spain): upper crustal shear-wave velocity structure and radial anisotropy using seismic ambient noise.

Description

Figure S1 shows examples of sequential stacks of DCCFs and illustrates the stabilization of the dispersion measurements as the number of stacked DCCFs increase and the uncertainty of the velocity determinations. Figure S2 and S3 exemplify the recovery of three synthetic chequerboard models by the Rayleigh and Love inter-station raypaths, respectively. Figure S3 displays all the S-wave inverted models at each grid node and the sensitivity kernels of the inversions.

List of figure captions

Figure S1. Examples of stacks of sets of 30, 60, 90 and all the available daily cross-correlation functions for the CAST-OLES and E150-E151 inter-station paths (left panels). The central panels display the dispersion curves computed from the stacks of the left panels. The right panels show the dispersion measurements obtained from 10 stacks calculated from the randomly selected 75 per cent of all the available DCCFs for a inter-station path.

Figure S2. Recovery of synthetic chequerboard models with three different cell sizes (20x20 km, 30x30 km and 40x40 km) from the Z-Z inter-station raypaths at 4, 8 and 12 s periods. Triangles symbolize the location of seismic stations in Fig. 2.

Figure S3. Recovery of synthetic chequerboard models with three different cell sizes (20x20 km, 30x30 km and 40x40 km) from the T-T inter-station raypaths at 4, 8 and 12 s periods. Triangles symbolize the location of seismic stations in Fig. 2.

Figure S4. Vsv and Vsh velocity models (left panels) inverted for each node of the grid (grey lines) and reference velocity models (black lines) obtained from the inversion of the average dispersion curves of the entire study area (Figs. 3e and 3f). Rayleigh and Love wave depth sensitivity kernels of the inversions (right panels).

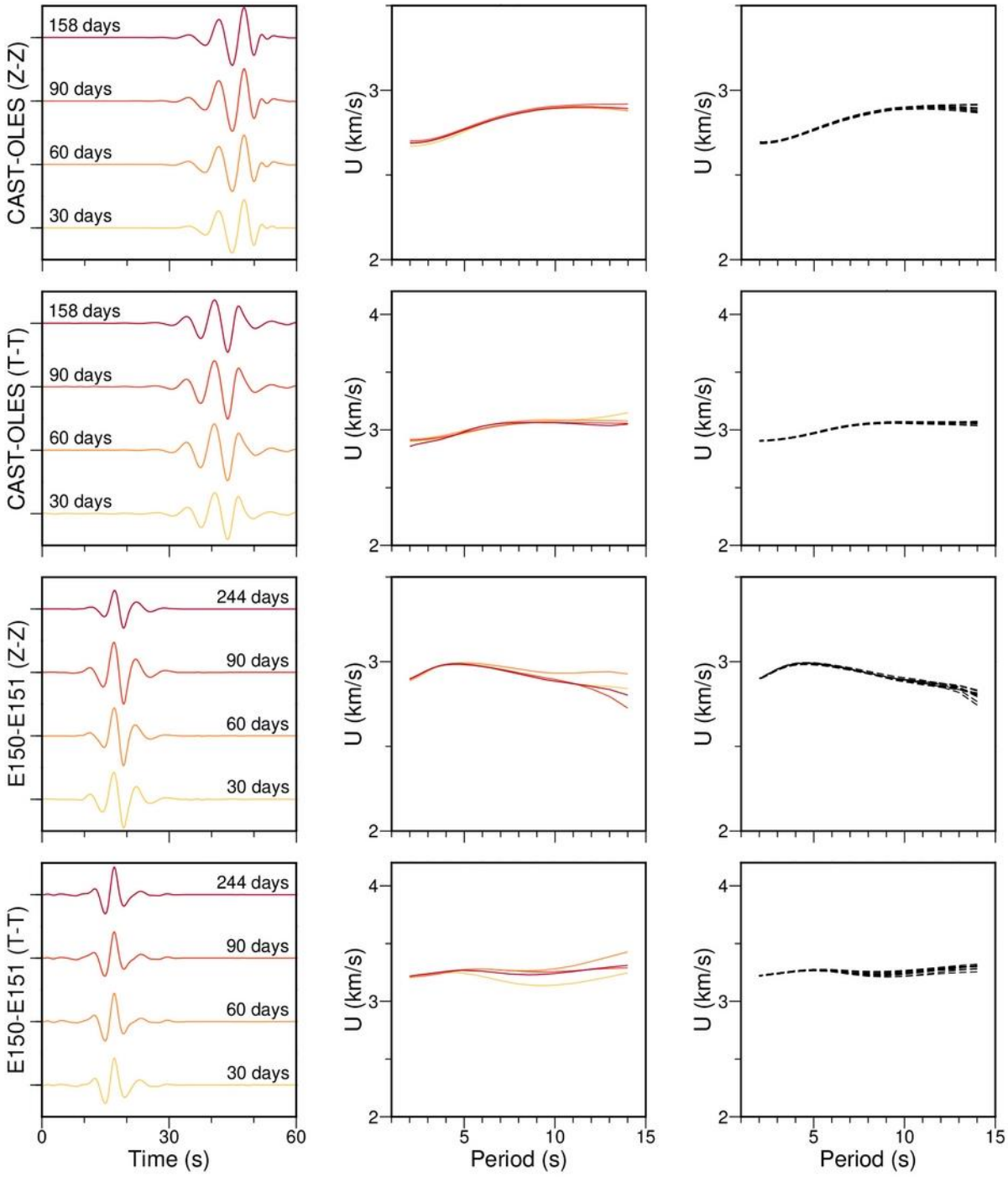

Figure S1. Examples of stacks of sets of 30, 60, 90 and all the available daily cross-correlation functions for the CAST-OLES and E150-E151 inter-station paths (left panels). The central panels display the dispersion curves computed from the stacks of the left panels. The right panels show the dispersion measurements obtained from 10 stacks calculated from the randomly selected 75 per cent of all the available DCCFs for a inter-station path.

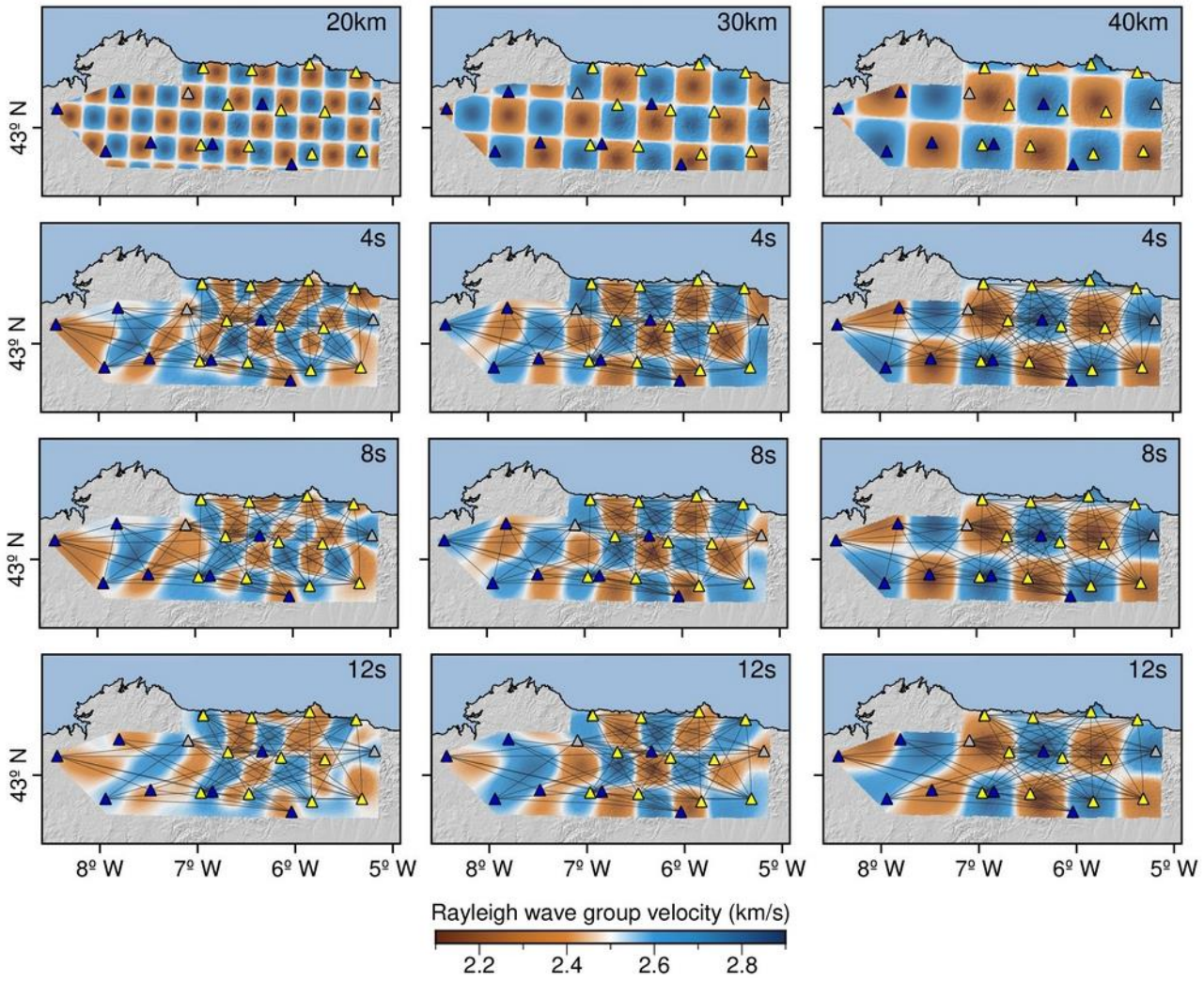

Figure S2. Recovery of synthetic chequerboard models with three different cell sizes (20x20 km, 30x30 km and 40x40 km) from the Z-Z inter-station raypaths at 4, 8 and 12 s periods. Triangles symbolize the location of seismic stations in Fig. 2.

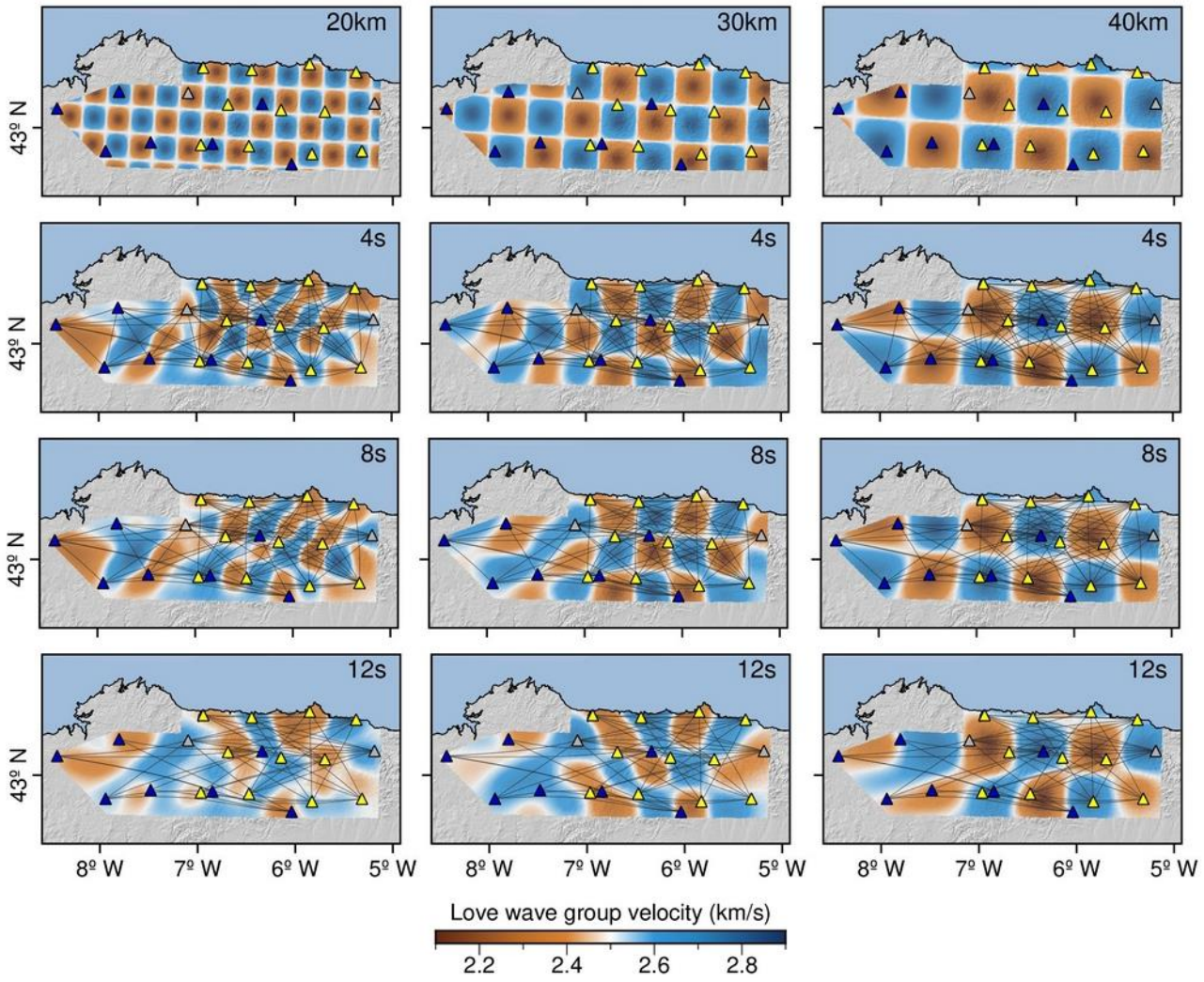

Figure S3. Recovery of synthetic chequerboard models with three different cell sizes (20x20 km, 30x30 km and 40x40 km) from the T-T inter-station raypaths at 4, 8 and 12 s periods. Triangles symbolize the location of seismic stations in Fig. 2.

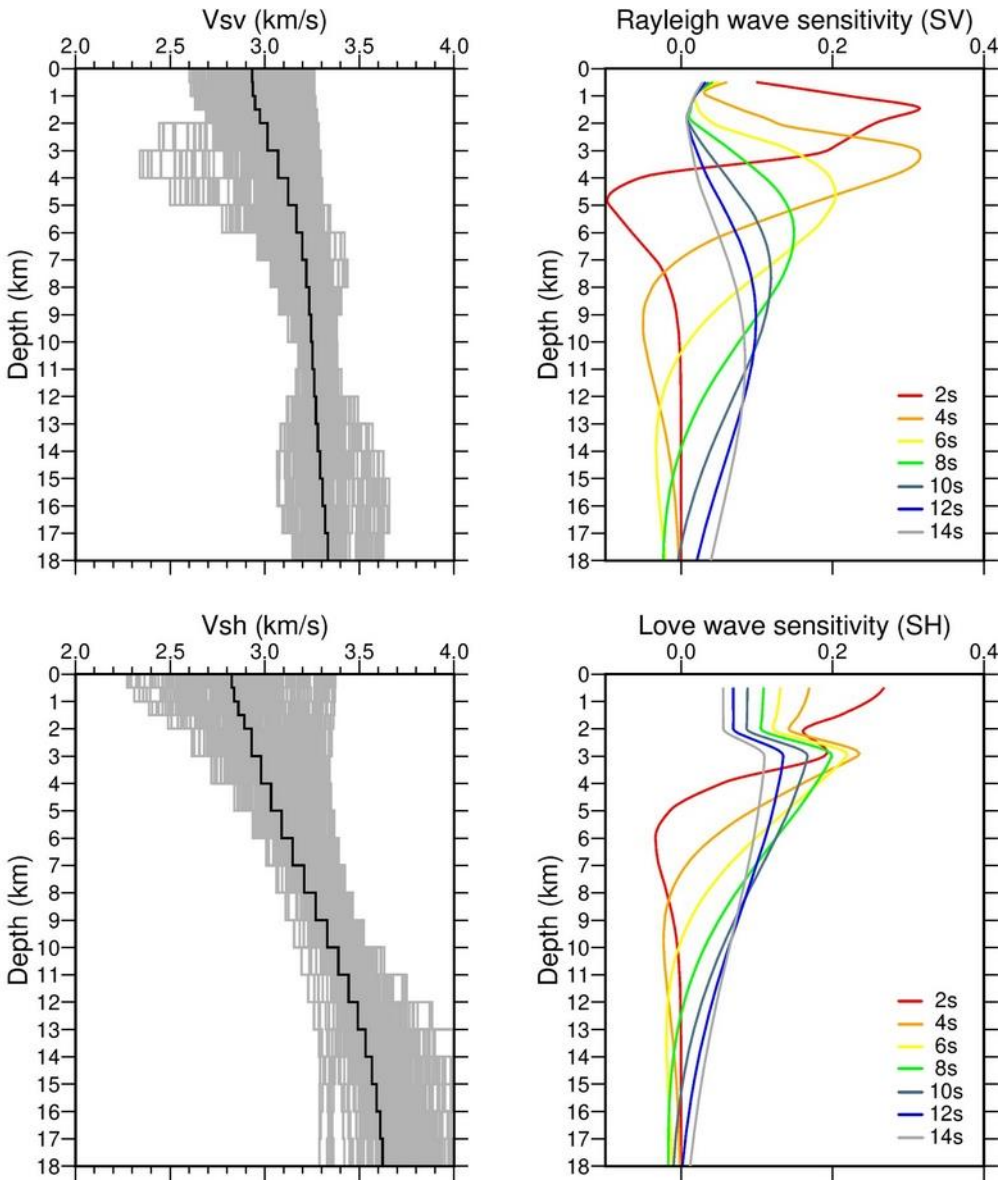

Figure S4. Vsv and Vsh velocity models (left panels) inverted for each node of the grid (grey lines) and reference velocity models (black lines) obtained from the inversion of the average dispersion curves of the entire study area (Figs. 3e and 3f). Rayleigh and Love wave depth sensitivity kernels of the inversions (right panels).